

SECOND HARMONIC IMAGING FROM PULSE-ECHO SIGNALS OF CONTRAST-ASSISTED ULTRASOUND

Tosaporn Nilmanee^{1*}, Surapon Thienmontri², Nattha Jindapetch² and Pornchai Phukpattaranont²

Received: Jun 14, 2007; Revised: Oct 25, 2007; Accepted: Oct 26, 2007

Abstract

Increasing interest in extending the diagnostic capabilities of medical ultrasound imaging by utilizing ultrasound contrast agents (UCAs) has heightened the need for suitable harmonic separation models. This article describes the second harmonic frequency characteristic and second harmonic image generation from pulse-echo signals of UCA. Based on the differences in frequency of ultrasound data from two different media, ultrasound signals are classified into two classes, i.e., UCA and tissue. We show the frequency characteristic of the UCA signals from an *in vivo* target to demonstrate this nonlinear behavior. Then, the difference in frequency components of the UCA and tissue data is used as a reference to design a linear bandpass filter (LBF) in order to separate the UCA signals from tissue echoes. The LBF is designed using the Parks-McClellan algorithm. We find that the appropriate fractional bandwidth (*FB*) and stopband attenuation of the LBF are 15% - 25% and 40 - 50 dB, respectively. The imaging quality for medical ultrasound purposes, by utilizing the information from the frequency contents of contrast-assisted ultrasound data, has been improved. Results show that the images produced from the output signals of the optimal LBF are superior to the original B-mode images both in terms of contrast and spatial resolution.

Keywords: Ultrasound contrast agents, harmonic imaging, linear bandpass filter

Introduction

State-of-the-art ultrasonic imaging modalities utilize nonlinear oscillation from ultrasound contrast agents (UCAs) to enhance diagnostic capabilities in medical applications (Frinking *et al.*, 2000). Radial oscillations of microbubbles due to compressional and rarefactional cycles of the applied pressure are not symmetrical

resulting in harmonic echoes, i.e., the fundamental (f_0) and its higher multiple frequencies ($2f_0, 3f_0, \dots$) (de Jong *et al.*, 1994a, 1994b). These harmonic frequencies, especially the second harmonic, are significantly higher than those from the surrounding tissue and can be exploited in the separation of the UCA echoes from the

¹ 22 M.1 Namnoi, Hatyai, Songkhla, 90110, Thailand, Mobile Phone: 08-6612-9299. E-mail: tj_spy@hotmail.com

² Department of Electrical Engineering, Faculty of Engineering, Prince of Songkla University, Hatyai, Songkhla, 90112, Thailand, Tel.: 0-7428-7045; Fax.: 0-7445-9395, E-mail: surapon.t@psu.ac.th, nattha.s@psu.ac.th, pornchai.p@psu.ac.th

* Corresponding author

surrounding medium. Consequently, many reports of the improved diagnostic capabilities exploiting UCAs in clinical applications have been published (Cosgrove, 2006). Examples include improved discrimination between benign and malignant liver tumors (Ramnarine *et al.*, 2000), improved depiction of the vascularity of cancerous tumors occurring in the liver (Tanaka *et al.*, 1995), and enhanced assessment of myocardial perfusion (Frischke *et al.*, 1997).

In this paper, we demonstrate the difference in frequency characteristic of contrast-assisted ultrasound signals from the surrounding tissue echoes using an *in vivo* target. Then, we employ the frequency difference to design an optimal linear bandpass filter (LBF) in order to separate the UCA signals from the surrounding tissue echoes. The finite-impulse response (FIR) filter is more appropriate than the infinite-impulse response (IIR) filter in our application because it can be designed with exactly linear phase and it is inherently stable (Er *et al.*, 2003). There are many techniques for FIR filter design. The window method is one of the earliest and simplest techniques. The filter coefficient can be obtained in closed form without the need for solving complex optimization problems. Hence, the design time is very short. However, it is not optimal in any sense. Frequency sampling method, which can be used in frequency domain directly and effectively, is one of the usual methods in FIR filter design. But it is difficult to determine the value of transition band samples and yields low stopband attenuation. On the other hand, the most widely used design algorithm is the Park-McClellan's method, which affords the best control over band limits and high stopband attenuations. For a given set of frequency selective specifications, the Park-McClellan algorithm tends to be of lower order than filter designed with the windowed and frequency-sampled method (Schilling and Harris, 2005). As a consequence, the Parks-McClellan algorithm is selected for the LBF design. In the performance evaluation, fractional bandwidth (*FB*) and stopband attenuation of the LBF are varied and investigated in order to achieve the best filter for enhancing imaging

quality both in terms of contrast and spatial resolution.

Materials and Methods

Experimental Setup and Data Acquisition

The experiment was conducted *in vivo* on a guinea pig. Bolus injections of SonoVue™ (Bracco Research SA, Geneva, Switzerland), a UCA consisting of sulphur hexafluoride gas bubbles coated by a flexible phospholipidic shell, were administered with a concentration of 0.01 mL/kg. Figure 1 shows the imaging setup for the guinea pig's kidney. Three-cycle pulses at 1.56 MHz were transmitted with a mechanical index of 0.158 to scan the kidney of the guinea pig. Radio frequency (RF) data were acquired with 16-bit resolution at 20-MHz sampling frequency. In addition, all RF data were recorded and saved for off-line processing by the Technos MPX ultrasound system (ESAOTE S.p.A, Genoa, Italy) with a convex array probe (CA430E; ESAOTE S.p.A, Genoa, Italy).

Power Spectrum

After data acquisitions, we determined the power spectrum of RF A-lines from the UCA regions compared with those from the tissue regions. Power spectrum of A-line data was obtained using the periodogram method with a weighted sequence. The multiplication of the weighted sequence, i.e. window, in the time domain is convolution in the frequency domain, so some resolution gets lost by smearing and spectral leakage. However, the trend of the signal's estimated power spectral density (PSD) can be enhanced by the use of a window function with faster decaying side-lobes. The expression used to calculate the power spectrum is given by

$$S(e^{j\omega}) = \frac{\left| \frac{1}{n} \sum_{i=1}^n w_i x_i e^{-j\omega i} \right|^2}{\frac{1}{n} \sum_{i=1}^n |w_i|^2} \quad (1)$$

where $S(e^{j\omega})$ is a power spectrum, $[x_1, \dots, x_n]$ is a

signal sequence, and $[w_1, \dots, w_n]$ is a weighted sequence. This expression is an estimate of the power spectrum of the signal sequence $[x_1, \dots, x_n]$ weighted by the window sequence $[w_1, \dots, w_n]$. A periodogram uses an n-point FFT to compute the PSD as $S(e^{j\omega})$ where F is a sampling frequency. Twenty-one segments of A-lines from the UCA and tissue regions were used to determine power spectra. Each segment consisted of 201 samples of data. A Hanning window was chosen as the weighted signal sequence in this paper. An n-point symmetric Hanning window can be expressed as

$$w[k+1] = 0.5 \left(1 - \cos \left(2\pi \frac{k}{n+1} \right) \right), k = 0, \dots, n-1 \quad (2)$$

Linear Bandpass Filter (LBF)

In this paper, we use the Parks-McClellan algorithm (Parks and McClellan, 1972) to design a linear bandpass filter (LBF). The designed filters exhibit an equiripple behavior in their frequency response, and hence are also known as equiripple filters. The parameters for the LBF design, i.e. fractional bandwidth and stopband

attenuation, are chosen to maximize the difference in the spectra of echo signals from the UCA and tissue regions. The LBF with optimal parameters should enhance the UCA components but suppress the tissue signals. Parameters to be considered for the design of the LBF are shown in Figure 2. The fractional bandwidth of the LBF can be obtained by

$$FB = \frac{2f_B}{f_C} \times 100\% \quad (3)$$

where FB is a fractional bandwidth, f_B is one-half of a defined passband in the filter specification, and f_C is a center frequency. In addition, stopband attenuation is defined in terms of dB below the passband of the filter. Signal outputs from the optimal LBF are used to make a gray-level image, which provides better quality for medical diagnosis.

Contrast Resolution

We measured the contrast resolution of images using a contrast-to-tissue ratio (CTR), which is given by (Al-Mistarihi *et al.*, 2004a, 2004b)

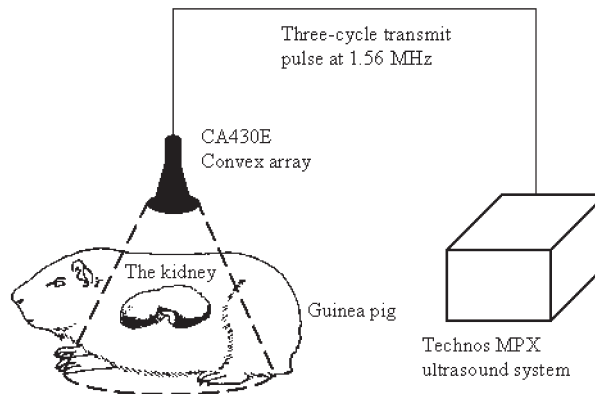


Figure 1. The imaging setup for the guinea pig’s kidney

$$CTR = 10 \log \frac{\bar{P}_C}{\bar{P}_T} \quad (4)$$

where \bar{P}_C and \bar{P}_T are the average power of signals in the UCA and tissue regions, respectively. The average power is obtained by

$$\bar{P} = \frac{1}{IJ} \sum_{i=1}^I \sum_{j=1}^J x_{ij}^2 \quad (5)$$

where x_{ij} is the signal in the reference region. We use CTR as a measurement of the LBF's capability in extracting second harmonic components. The appropriate LBF for producing a gray-level image with enhanced quality should provide a high CTR value.

Results and Discussion

Frequency Characteristic

The gray image of the guinea pig's kidney is shown in Figure 3(a) with a 50 dB dynamic range. The reference tissue and UCA regions used for calculation of the power spectra are on the left and right white boxes, respectively. Each

region consists of 21 A-line pulse-echo signals. To investigate more details of the frequency characteristic of pulse-echo signals, we show the average spectra and standard deviation (SD) of 21 A-lines from the tissue and UCA regions in Figure 3(b) and (c), respectively. We can see that every A-line signal from the UCA region exhibits the second harmonic frequency. On the contrary, the A-line signal from the tissue region contains only the fundamental frequency. Average spectra determined from 21 A-line signals of the tissue and UCA regions on the left and right boxes of Figure 3(a) are shown in Figure 3(d) using dotted and solid lines, respectively. We can see that the harmonic spectrum of the UCA echoes (solid line) between 2.5 and 4.0 MHz band are broader than those from tissue echoes (dotted line). This result obviously shows the fundamental and second harmonic frequency generation due to the UCAs. On the other hand, the signals from the tissue regions contain only the transmitted fundamental frequency.

Stopband Attenuation

We can clearly see in Figure 3(d) that the UCA components are higher than the tissue components in the frequency range between 2.5 and 4.0 MHz. Based on this observation, the

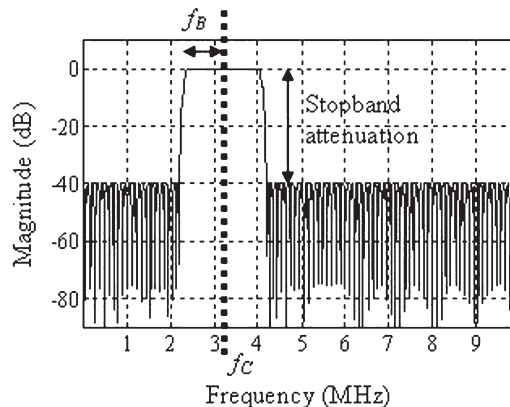


Figure 2. Two parameters considered in the design of an optimal LBF: Fractional band width (FB) and stopband attenuation

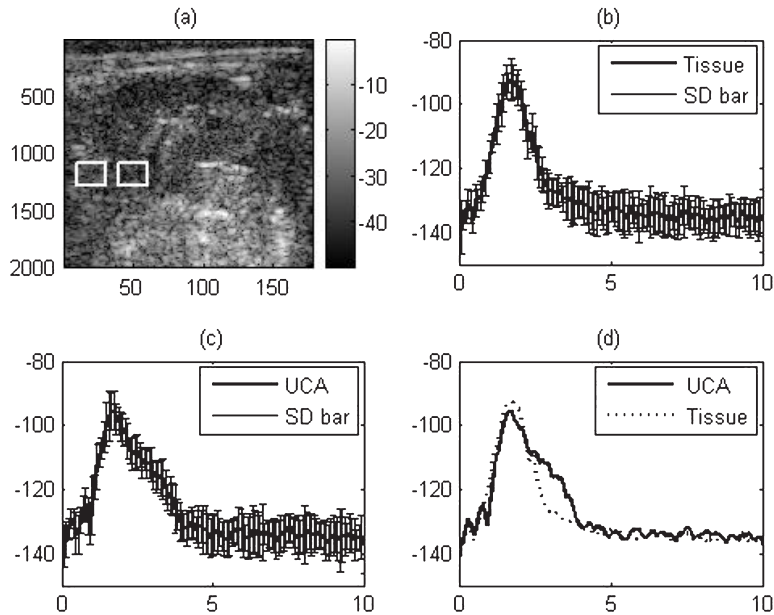


Figure 3. (a) B-mode image of the guinea pig's kidney (b) Average spectra and standard deviation (SD) of 21 A-line signals from the tissue region. (c) Average spectra and SD of 21 A-line signals from the UCA region. (d) Average spectra of tissue and UCA signals from the left and right boxes of Figure 3(a)

center frequency is selected to be 3.2 MHz for all designs of the LBF in this paper. In order to investigate the appropriate stopband attenuation, we designed the LBF with a fixed *FB* of 12.5%. The gray-level images of the guinea pig's kidney resulting from various stopband attenuations with fixed fractional bandwidth at 12.5% are shown in Figure 4. Images after filtering with the LBF produced from the stopband attenuation of 20, 30, 40, and 50 dB are shown in Figure 4(a), (b), (c), and (d), respectively. It is shown that images in Figure 4(c) and (d) have a comparable contrast resolution and are better than those from images in Figure 4(a) and (b). We can clearly visualize the kidney shape and large vascular structures inside the kidney. In addition, *CTR* values from images in Figure 4(a), (b), (c), and (d) are 2.0, 8.5, 11.8, and 12.7 dB, respectively. These are in agreement with the

visualized inspection.

Fractional Bandwidth

Figure 5 shows gray-level images from the LBF with a different fractional bandwidth at the fixed stopband attenuation of 40 dB. Images after filtering with the LBF produced from the *FB* of 10%, 15%, 25%, and 50% are shown in Figure 5(a), (b), (c), and (d), respectively. It can be seen that the LBF with *FB* from 10% to 25% are appropriate for enhancing imaging quality in terms of contrast resolution. However, spatial resolution is improved when the *FB* of the LBF increases. In other words, the LBF with *FB* 25% provides the best image in terms of spatial resolution. The *CTR* values of images in Figure 5(a), (b), (c), and (d) are 11.2, 11.4, 11.0, and 2.8 dB, respectively. They agree well with the visualization.

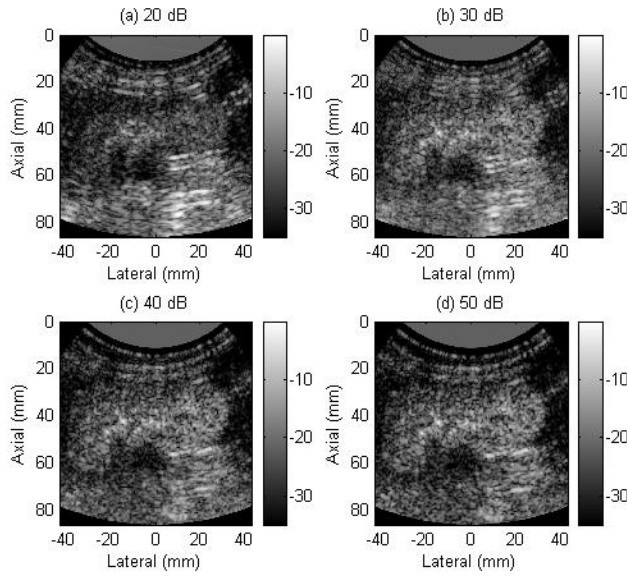


Figure 4. Gray-level images of the guinea pig's kidney from signals after filtering with the LBF by varying stopband attenuation to be 20, 30, 40, and 50 dB. FB is fixed at 12.5%. The *CTR* values from the images in Figure 4(a), (b), (c), and (d) are 2.0, 8.5, 11.8, and 12.7 dB, respectively

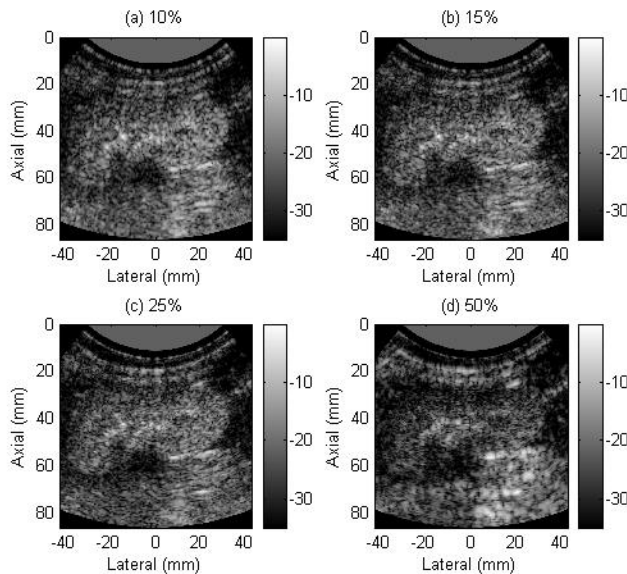


Figure 5. Gray-level images of the guinea pig's kidney from signals after filtering with the LBF by varying *FB* to be 10, 15, 25, and 50%. Stopband attenuation is fixed at 40 dB. The *CTR* values of the images in Figure 5(a), (b), (c), and (d) are 11.2, 11.4, 11.0, and 2.8 dB, respectively

Conclusions

We demonstrated the nonlinear properties from the interaction between the UCA and transmitted acoustic energy. The second harmonic frequency of pulse-echo signals from the UCA region is significantly higher than those from the surrounding tissue region. The imaging quality of medical ultrasound images can be enhanced by employing these second harmonic components. Gray-level images produced using the LBF with optimal fractional bandwidth (15 - 25%) and stopband attenuation (40 - 50 dB) are better than the original B-mode images both in terms of contrast and spatial resolution. We also explored the effects of filter ripples. It turns out that passband ripples have very slight effects to the imaging quality. However, the lower passband ripple results in the higher filter length. This leads to more computational complexity. Consequently, the passband ripple of approximately 0.5 dB is suggested for contrast-assisted ultrasonic imaging.

Acknowledgement

The authors thank ESAOTE S.p.A, Genova, Italy for supporting the *in vivo* data used in this paper.

References

- Al-Mistarihi, M.F., Phukpattaranont, P., and Ebbini, E.S. (2004a). A two-step procedure for optimization of contrast sensitivity and specificity of Post-Beamforming Volterra Filters. Proceedings of the 2004 IEEE International Ultrasonics Symposium; August 23-27, 2004; Montreal, Canada, p. 978-981.
- Al-Mistarihi, M.F., Phukpattaranont, P., and Ebbini, E.S. (2004b). Post-beamforming third-order Volterra filter (ThOVF) for pulse-echo ultrasonic imaging. Proceedings of the 2004 IEEE International Conference on Acoustics, Speech, and Signal Processing; May 17-21, 2004; Montreal, Canada, p. 97-100.
- Cosgrove, D. (2006). Ultrasound contrast agents: An overview. *Eur. J. Radiol.*, 60:324-330.
- de Jong, N., Cornet, R., and Lancee, C.T. (1994a). Higher harmonics of vibrating gas filled microspheres. Part one: Simulations. *Ultrasonics*, 32(6):447-453.
- de Jong, N., Cornet, R., and Lancee, C.T. (1994b). Higher harmonics of vibrating gas filled microspheres. Part two: Measurements. *Ultrasonics*, 32(6):455-459.
- Er, M.H., Antoniou, A., Smith, L.M., Bomar, B.W., Lim, Y.C., and Saramaki, T. (2003). In: *The Circuits and Filters Handbook*. Chen W.K., (eds). CRC Press, NY, p. 2,603-2,677.
- Feinstein, S.B., Shah, P.M., Bing, R.J., Meerbaum, S., Corday, E., Chang, B.L., Santillan, G., and Fujibayashi, Y. (1984). Microbubble dynamics visualized in the intact capillary circulation. *J. Am. Coll. Cardiol.*, 4: 595-600.
- Frinking, P.J.A., Bouakaz, A., Kirkhorn, J., Ten Cate, F.J., and de Jong, N. (2000). Ultrasound contrast imaging: current and new potential methods. *Ultrasound in Medicine & Biology*, 26(6):965-975.
- Frischke, C., Lindner, J.R., Wei, K., Goodman, N.C., Skyba, D.M., and Kaul, S. (1997). Myocardial perfusion imaging in the setting of coronary artery stenosis and acute myocardial infarction using venous injection of a second-generation echocardiographic contrast agent. *Circulation*, 96(3):959-967.
- Parks, T.W. and McClellan, J.H. (1972). Chebyshev approximation for non-recursive digital filters with linear phase. *IEEE Trans. Circuits Theory*, 19:189-194.
- Ramnarine, K.V., Kyriakopoulou, K., Gordon, P., McDicken, N.W., McArdle, C.S., and Leen, E. (2000). Improved characterization of focal liver tumours: dynamic power doppler imaging using NC100100 echo-enhancer. *Eur. J. Ultrasound*, 11(2):95-104.
- Schilling, R.J. and Harris, S.L. (2005). Fundamentals of digital signal processing using

- matlab. Thomson, p. 427-495.
- Tanaka, S., Kitamra, T., Yoshioka, F., Kitamura, S., Yamamoto, K., Ooura, Y., and Imaoka, T. (1995). Effectiveness of galactose based intravenous contrast medium on color doppler sonography of deeply located hepatocellular carcinoma. *Ultrasound in Medicine & Biology*, 21(2):157-160.